Deep phenotyping of nodal T-cell lymphomas reveals immune alterations and therapeutic targets

Pierre Stephan,[1] Jimmy Perrot,[2] Allison Voisin,[1] Maud Barbery,[1] Thibault Andrieu,[1] Maxime Grimont,[1] Julie Caramel,[1] Mathilde Bardou,[2] Garance Tondeur,[2] Edoardo Missiaglia,[3] Philippe Gaulard,[4] François Lemmonier,[4] Laurence de Leval,[3] Emmanuel Bachy,[2,5] Pierre Sujobert,[2,5] Laurent Genestier,[5] Alexandra Traverse-Glehen[2] and Yenkel Grinberg-Bleyer[1]

[1]Cancer Research Center of Lyon, UMR INSERM 1052, CNRS 5286, Université Claude Bernard Lyon 1, Labex DEV2CAN, Centre Léon Bérard, Lyon, France; [2]Centre Hospitalier Lyon Sud and Université Claude Bernard Lyon-1, Pierre-Bénite, France; [3]Institute of Pathology, Department of Laboratory Medicine and Pathology, Lausanne University Hospital and Lausanne University, Lausanne, Switzerland; [4]AP-HP, Henri Mondor Hospital, Pathology Department, Créteil, France, and University Paris Est Créteil, INSERM, IMRB, Créteil, France and [5]Centre International de Recherche en Infectiologie (CIRI), Team Lymphoma Immuno-Biology, UMR INSERM U1111, CNRS 5308, Université Claude Bernard Lyon I, ENS de Lyon, Lyon, France

Correspondence: Y. Grinberg-Bleyer
yenkel.grinberg-bleyer@inserm.fr

Received: October 16, 2023.
Accepted: May 17, 2024.
Early view: May 30, 2024.

https://doi.org/10.3324/haematol.2023.284448

Abstract

Whereas immunotherapies have revolutionized the treatment of different solid and hematologic cancers, their efficacy in nodal peripheral T-cell lymphomas (PTCL) is limited, due to a lack of understanding of the immune response they trigger. To fully characterize the immune tumor microenvironment (TME) of PTCL, we performed spectral flow cytometry analyses on 11 angioimmunoblastic T-cell lymphomas (AITL), 7 PTCL, not otherwise specified (PTCL, NOS) lymph node samples, and 10 non-tumoral control samples. The PTCL TME contained a larger proportion of regulatory T cells and exhausted CD8$^+$ T cells, with enriched expression of druggable immune checkpoints. Interestingly, CD39 expression was up-regulated at the surface of most immune cells, and a multi-immunofluorescence analysis on a retrospective cohort of 43 AITL patients demonstrated a significant association between high CD39 expression by T cells and poor patient prognosis. Together, our study unravels the complex TME of nodal PTCL, identifies targetable immune checkpoints, and highlights CD39 as a novel prognostic factor.

Introduction

Peripheral T-cell lymphomas (PTCL) are highly heterogeneous neoplasms derived from post-thymic T cells or mature natural killer (NK) cells, and represent 10-15% of non-Hodgkin lymphomas.[1] The two most common subtypes in Western countries are angioimmunoblastic T-cell lymphomas (AITL) and peripheral T-cell lymphomas, not otherwise specified (PTCL, NOS). Malignant cells in AITL are predominantly CD4$^+$CD8$^-$ and characterized by the expression of T-follicular helper cell (TFH) markers such as ICOS or PD-1.[2] PTCL, NOS display heterogeneous phenotypes that do not match any other category and represent about 20% of PTCL.[3] Despite advances in the understanding and classification of these neoplasms over the past decades, their prognosis remains poor, with a 5-year overall survival (OS) around 30%, fostering the need to identify new therapeutic targets. Moreover, although immune checkpoint inhibitors that target inhibitory receptors, such as PD-1/PD-L1 blocking agents, have been successfully used in some hematologic malignancies,[4,5] their clinical benefits in nodal PTCL are relatively modest,[6,7] and several cases of hyperprogression have even been reported in patients with different PTCL,[6,8] likely due to the expression of PD-1 by neoplastic cells.[9]

Transposing checkpoint-blockade-based immunotherapies to nodal PTCL has been hindered by our poor understanding of the types and phenotypes of immune cells recruited in response to these tumors. Studies focusing on the contribution of the tumor microenvironment (TME) to PTCL progression reported that monocytes, as well as immunosuppressive CD163$^+$ macrophages, were suggested to promote a worsening of the disease,[10,11] whereas high levels of B cells and dendritic cells (DC) and a high CD8/CD4 T-cell ratio were associated with better survival,[12,13] although these latter findings have recently been challenged.[14] Though generally of poor prognosis in most cancers,[15] the proportion and prognostic value of immunosuppressive Foxp3$^+$ regulatory T cells in PTCL are still unclear.[16,17] Finally, a recent study using Cytof and scRNA-seq approaches revealed the ex-

pression of exhaustion markers by tumor-infiltrating CD8$^+$ T cells, as well as perturbations in the B-cell compartment of patients with AITL.[18] In this study, we aimed to bridge this knowledge gap and extensively characterize the phenotype of immune cells recruited in response to PTCL.

Methods

Samples for spectral flow cytometry analyses

Frozen lymph node (LN) cell suspensions from 18 PTCL samples, collected at diagnosis, were obtained through the CeVi_Collection Project from the CALYM Carnot Institute (Lyon, France). Samples were collected as part of an RIPH3 project (ID RCB 2020-A02273-36, validated by the CPP Ile de France V on November 26, 2020; N. 20.07.28.49748). Reactive LN suspensions were obtained from the biological resource center of Lyon-Sud Hospital (agreement CRB BB-0033-00046). Tissues were assessed by the pathology department, and cancer diagnosis was excluded through pathological evaluation and absence of T or B clonality. All adult patients (aged ≥18 years) gave their written informed consent on the secondary use of their samples for research. The clinical and biological data of the patients were collected retrospectively. Their characteristics are presented in *Online Supplementary Tables S1 and S2*.

Blood samples from healthy volunteers were obtained through the Etablissement Français du Sang (EFS). Peripheral blood mononuclear cells (PBMC) were isolated by Ficoll density gradient centrifugation, and red blood cells were lysed with ammonium-chloride-potassium lysis buffer. Tonsils obtained anonymously from 5 donors that had undergone tonsillectomy were used as a control (Clinique du Parc, Lyon; agreement N. 1A16502305468). Tonsils were reduced to cell suspensions by mechanical disruption followed by enzymatic digestion with 2 mg/mL collagenase-D (Roche) and 20 U/mL DNase (Sigma). The resulting cell suspensions were filtered, washed, and frozen.

Samples for multi-immunofluorescence analyses

Forty-three tissue blocks of formalin-fixed and paraffin-embedded (FFPE) AITL samples, collected at diagnosis, were obtained from the Department of Pathology at the Lyon-Sud Hospital. This study was performed according to the principles of the Declaration of Helsinki. Patients had provided informed consent. The study was approved by the local ethics committee (MR-004 N. 23-5211). Clinical and biological data of the patients were collected retrospectively. A summary of the data is presented in *Online Supplementary Tables S3 and S4*.

Flow cytometry

A total of 1 million live cells were stained through successive incubation steps with dyes and antibodies (Ab). The complete list of Ab and their final concentration can be found in *Online Supplementary Table S5*. Acquisition was performed on an Aurora Spectral Cytometer (Cytek). Analyses were carried out using the OMIQ software (Dotmatics) (www.omiq.ai). Details on the experimental protocol and analyses can be found in the *Online Supplementary Methods*; the number of cells analyzed in each subset is detailed in *Online Supplementary Tables S6 and S7*.

Tissue micro-arrays, multi-immunofluorescence protocol, and data analysis

Representative tumor areas were selected on Hematoxylin & Eosin slides by an experienced pathologist. A 4-plex mIF assay (CD3, CD8, CD39 and DAPI) was performed using a modified 7-color TSA protocol template. Slides were imaged using the Vectra Polaris spectral imaging system (Perkin Elmer). Scans were visualized with the Phenochart software. Cell segmentation and phenotypes were identified by InForm version 2.4.8 (Akoya Biosciences). Parameters were analyzed using R version 4.2.1. More detailed information can be found in the *Online Supplementary Methods*.

Statistical analyses

Statistics were performed using GraphPad Prism Software v9 and R version 4.2.1. Kruskall-Wallis or two-way ANOVA tests were used for FACS data, unless otherwise stated. Statistical analyses for comparison between clusters established by the FlowSOM algorithm, were carried out using the edgeR package. Progression-free survival (PFS) was calculated from the date of diagnosis to the date of progression, relapse, or death from any cause. OS was calculated from the date of diagnosis to the date of death from any cause. Survival estimates were calculated with the Kaplan-Meier method. Survival distributions were compared with the log-rank test, and Cox proportional hazard regression models were used to estimate hazard ratios and associated 95% Confidence Intervals.

Results

Peripheral T-cell lymphoma-specific immune cell populations identified through deep immunophenotyping

To document immune phenotypes associated with PTCL, we designed a 33-color flow cytometry panel to identify different innate and adaptive subsets in a single tube, namely DC, macrophages, NK and B cells, and a number of markers to distinguish subsets of T cells. Moreover, activation, proliferation, and exhaustion of these populations were determined using different intracellular and surface markers (Table 1, *Online Supplementary Table S5*). We applied this immunophenotyping panel to LN cell suspensions obtained from 18 nodal PTCL patients at diagnosis (11 AITL and 7 PTCL, NOS) (*Online Supplementary Tables S1* and *S2*), as well as 5 non-tumoral reactive LN, 5 tonsil samples, and 5 PBMC samples obtained from healthy donors. Of note,

PFS and OS of our PTCL cohort corroborated previous reports (*Online Supplementary Figure S1A*).

To identify disease-specific cell populations, we first normalized the data to attenuate the batch effect, concatenated all lymphoid tissue (tumoral LN, non-tumoral tonsil, reactive LN) samples, and carried out a series of unsupervised analyses. PBMC were not included in these analyses to avoid major changes in cell-type distribution (*data not shown*). Two-dimensional reduction through Uniform Manifold Approximation and Projection (UMAP) and computer-driven clustering through FlowSOM conducted on cell-type markers (CD3, CD4, CD8, CD56, TCRγδ, CD163, CD11c, CD20) identified 18 clusters, largely corresponding to classical immune lineages (T cells, NK cells, B cells, DC) (Figure 1A, B, *Online Supplementary Tables S6* and *S7*). Interestingly, this unsupervised analysis revealed a clear distinction between samples from PTCL patients and non-tumoral samples (Figure 1A, *Online Supplementary Figure S1B*). Specifically, we detected tissue-specific B-cell and T-cell clusters, and noted that DC (cluster 14) were higher in both AITL and PTCL, NOS samples compared to control LN or tonsil samples (Figure 1B). Two patient-specific clusters with aberrant phenotypes, namely cluster 13 ($CD3^+CD4^-CD8^-$) and cluster 7 ($CD3^+CD4^+CD20^+$) were differentially represented between NOS and AITL samples, though the proportions of the remaining cell subtypes were very similar. Supervised analyses based on traditional manual gating revealed a strong decrease in B cells in PTCL samples compared to non-tumoral tissues, and an increase in DC (Figure 1C, *Online Supplementary Figure S2*). $CD4^+$ and $CD8^+$ T cells were also more abundant in PTCL compared to tonsil samples, but not reactive LN. Of note, NK cells ($CD7^+CD56^+$) were slightly more abundant without reaching statistical significance.

To assess the putative link between the abundance of cell types and their proliferation, we measured Ki67 expression, and found a systematic increase in proliferating $CD4^+$ and $CD8^+$ T cells in malignant samples (Figure 1D). A trend toward B-cell proliferation was observed in PTCL, NOS samples compared to controls. This was not the case in AITL samples, probably because TFH features of tumor cells enhance B-cell activation, maturation, and proliferation.[19]

Analysis of $CD4^+$ T-cell subsets in peripheral T-cell lymphoma

Next, we analyzed the features of $CD4^+Foxp3^-$ conventional (Tconv) cells, that contained both transformed and normal cells, in PTCL compared to tonsils and reactive LN. Based on histological evaluation at diagnosis, all patients of our AITL cohort displayed a $CD3^+CD4^+CD8^-$ $Foxp3^-$ tumor cell phenotype, whereas 2 of our PTCL, NOS patients harbored a $CD3^+CD4^-CD8^-$ phenotype (Figure 1B, *Online Supplementary Table S2*). We used UMAP and FlowSOM algorithms with T-cell markers, proliferation / activation proteins and checkpoint receptors as variables (Figure 2A). Cells were highly activated in all samples, with only a minority of $CD45RA^+$ naïve-like cells (Figure 2B). We identified 21 clusters, corresponding to cells expressing divergent levels of CD7/CD10, Ki67 and many checkpoints, including TFH markers, such as ICOS and PD-1. Strikingly, a series of clusters from PTCL samples were clearly separated from control samples on the UMAP, highlighting the fact that transformation deeply impacted the Tconv cell phenotype either in an intrinsic or extrinsic manner (Figure 2C). Indeed, control samples harbored significantly more classical $CD7^+PD\text{-}1^+ICOS^+CXCR5^+$ TFH cells than PTCL (clusters 5, 19, and 20), whereas AITL samples comprised discrete and specific phenotypes, including $CD10^+$ and/or $CD7^-$ cells as expected, but also showing high expression of LAG-3 (cluster 15), or OX-40 (cluster 8). In PTCL, NOS, we observed patient-specific clusters, such as a cytotoxic phenotype (patient 11, cluster 11) and a $TCR\gamma\delta^+$ malignancy (patient 20, cluster 2). Tconv cells from AITL patients were also highly heterogeneous, with variable expression of checkpoints (*Online Supplementary Figure S3A, B*). Because of this heterogeneity, hierarchical clustering failed to fully discriminate reactive LN from PTCL samples (*Online Supplementary Figure S3C*). Analysis through manual gating confirmed strong expression of PD-1 and ICOS in AITL (>50% cells expressing ICOS, PD-1 or both), but without reaching statistical significance. Interestingly, the proportion of $PD1^+ICOS^+$ double positive cells in PTCL, NOS samples was reduced compared to tonsils and AITL, showing that most cells did not adopt a full TFH-like phenotype (Figure 2D). Thus, in addition to TFH markers widely used for diagnosis, we show that $CD4^+$ T cells from AITL samples adopt a highly activated state, often characterized by heterogeneous expression of different checkpoint molecules.

Given that tumoral PTCL T cells can lose the expression

Table 1. Spectral flow cytometry panel.

Cell populations	General phenotype	Activation checkpoints	Inhibitory checkpoints
Live/dead	CD10	ICOS	PD-1
CD3	CXCR5	OX-40	CTLA-4
CD4	BCL6	4-1BB	TIM-3
CD7	Ki67	TNFR2	LAG-3
CD8	EOMES	DNAM-1	NKG2A
FOXP3	T-BET	-	CD39
CD56	GZMB	-	TIGIT
CD57	TCF-1	-	-
CD20	CD45RA	-	-
CD11c	-	-	-
CD163	-	-	-
TCRγδ	-	-	-

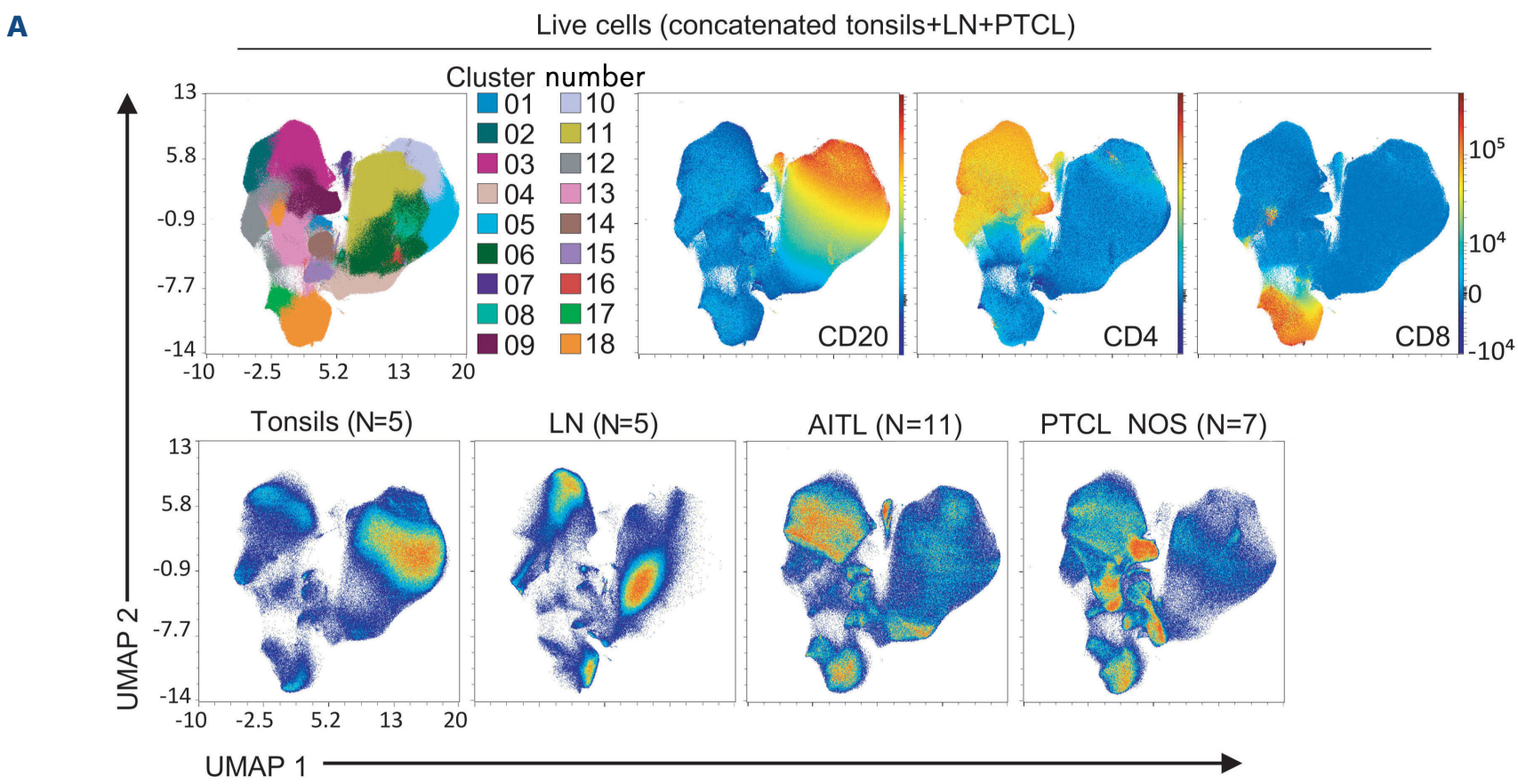

Figure 1. Perturbations in immune cell subsets in nodal peripheral T-cell lymphoma tissues. Samples were stained for FACS and analyzed using unsupervised clustering (A-B) and traditional supervised analyses (C, D) after manual gating on total live cells (see *Online Supplementary Figure S2*). (A) Uniform Manifold Approximation and Projection (UMAP) visualization, FlowSOM distribution of clusters and projection of selected markers in concatenated samples after random selection of an equal number of cells between each group: 5 tonsils, 5 reactive lymph nodes (LN), 11 angioimmunoblastic T-cell lymphomas (AITL), 7 peripheral T-cell lymphoma, not otherwise specified (PTCL, NOS). (B) Heatmap showing hierarchical clustering and expression (normalized across markers) of indicated markers in FlowSOM clusters, and their differential enrichment between groups. (C) Proportion of immune subsets using a supervised gating strategy. (D) Proportion of proliferating Ki67+ cells across cell populations. Mean + Standard Error of Mean is shown; each dot represents a sample. Kruskal-Wallis tests were used. DS: dendritic cells; FC: flow cytometry; FDR: false discovery rate; NK: natural killer cells. *P<0.05, **P<0.005, ***P<0.001, ****P<0.0001, ns: not significant. ^Patient-specific cluster.

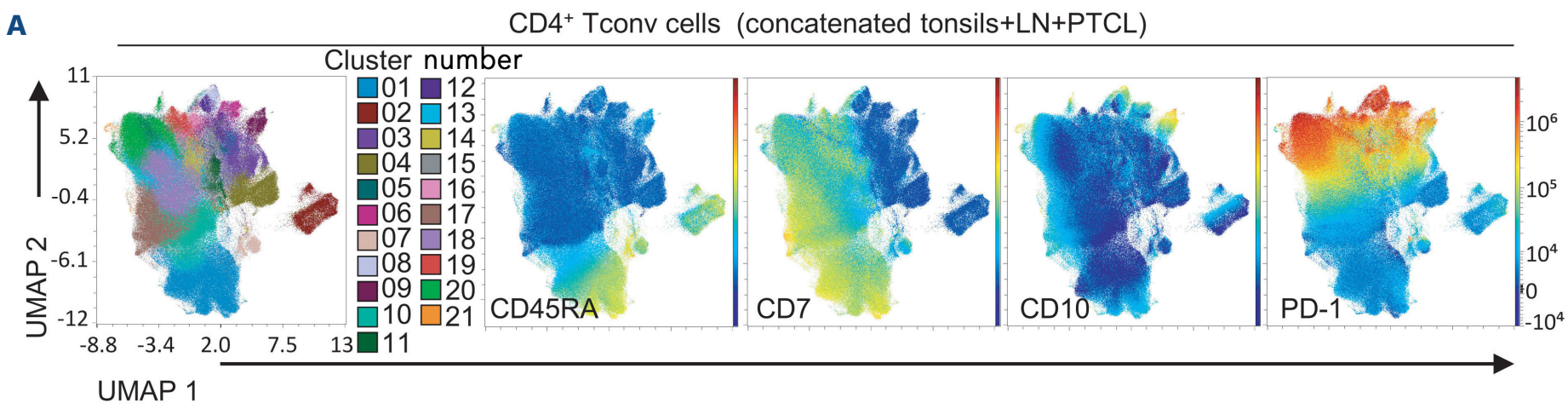

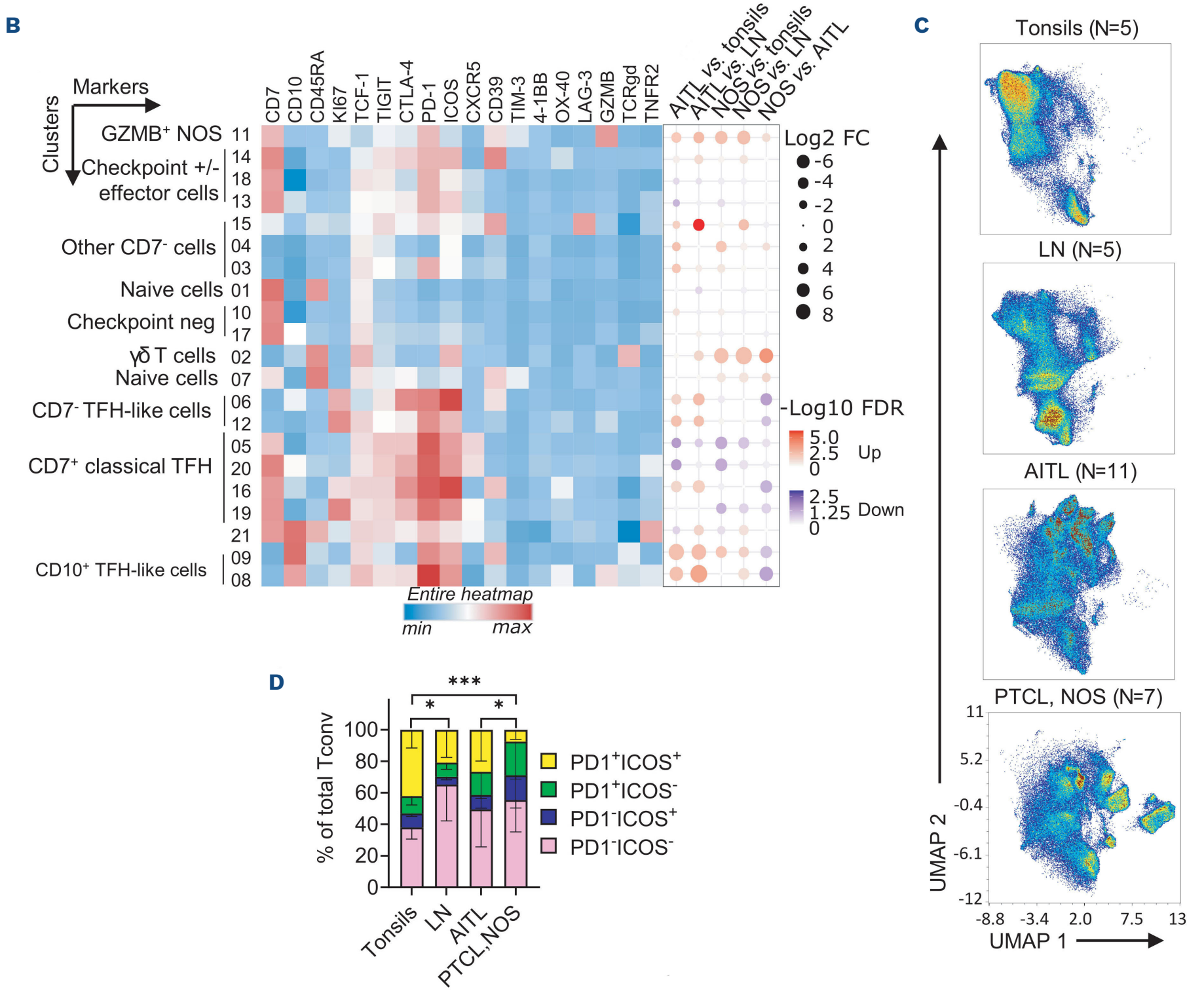

Figure 2. Diverse phenotypes of CD4⁺ conventional T cells in peripheral T-cell lymphoma. (A-D) Unsupervised clustering analyses following manual gating on live CD3⁺CD4⁺Foxp3⁻ conventional T cells (Tconv). (A) UMAP visualization, FlowSOM distribution of clusters and projection of selected markers in concatenated samples after random selection of an equal number of cells between each group. (B) Heatmap showing hierarchical clustering and expression (normalized across markers) of indicated markers in FlowSOM clusters, and their differential enrichment between groups. (C) Distribution of cells from each group on UMAP. (D) Proportion of PD-1 and ICOS-expressing Tconv cells upon manual gating. Mean ± Standard Error of Mean is shown. Two-way ANOVA tests were used; only the comparison of PD-1⁺ICOS⁺ cells between groups is shown. TFH: follicular helper cells; FC: flow cytometry; FDR: false discovery rate; LN: lymph nodes; AITL: angioimmunoblastic T-cell lymphoma; PTCL, NOS: peripheral T-cell lymphoma, not otherwise specified. *P<0.05, ***P<0.001.

of surface CD3 (sCD3), we also looked for aberrant cell phenotypes in the sCD3-negative compartment. Among the 23 clusters identified within these cells, we found, as expected, B cells, NK cells or DC (*Online Supplementary Figure S4A, B*). Interestingly, several other cell populations were more abundant in PTCL samples (*Online Supplementary Figure S4C*). These included cluster 5, retrieved in 2 patients, that matched a $CD4^+$ checkpoint$^+$ TFH-like phenotype, similar to that found in $sCD3^+$ Tconv cells; these were likely to be malignant. The cytotoxic phenotype of patient 11 was also found within a sCD3-negative cluster (cluster 3). In addition to this, we found 2 aberrant $CD4^-Foxp3^+CD39^+$ clusters (clusters 9 and 15) only found in patients 9 and 25, but which did not match the phenotype of their $sCD3^+$ counterpart (Figure 2B, D).

To further harness the complexity of these tumor cell phenotypes, we next analyzed each sample individually in order to ascertain that no rare cell cluster was overlooked. We specifically looked for clusters of cells presenting a non-classical phenotype, i.e., T cells harboring loss of CD7, gain of CD10, or aberrant expression of surface or intracellular proteins. This strategy led to the identification of putative neoplastic phenotypes in most, but not all, samples (*Online Supplementary Table S8*). Interestingly, in 3 PTCL, NOS samples, cell clusters exhibiting co-expression of PD-1 and ICOS could be found; thus, a diagnosis of nodal follicular helper T-cell lymphoma NOS could not be fully excluded in these cases. In line with our previous observations, we detected a very high heterogeneity between samples. Importantly, in about half of the cases, we found more than one aberrant phenotype, indicating that, as shown in many other cancers, PTCL are also prone to intra-tumor heterogeneity.

The data thus illustrate both the complexity of proper tumor-cell identification in nodal PTCL, and the perturbations of immune homeostasis in these diseases. This also warrants the use of additional tools (TRBC1 staining, TCR clonality at the single-cell level) to better understand the biology of nodal PTCL.

$Foxp3^+$ Treg cells are critical inhibitors of anti-tumor immunity. We detected a significant increase in the proportion of Treg cells among $CD4^+$ T cells in both AITL and PTCL, NOS compared to tonsil and LN samples (*Online Supplementary Figure S5A*). Based on classical activation markers and Treg cell hallmarks, 6 cell clusters were identified through FlowSOM, corresponding to $CD45RA^+$ naïve (cluster 6), $PD1^+ICOS^+$ TFR-like (cluster 4), $CD39^{bright}TIGIT^{high}$ (cluster 1) cells, as well as a subset with high expression of multiple Treg markers (cluster 2) (*Online Supplementary Figure S5B, C*). Cluster 5 was specific to patient PTCL, NOS 11. Of those populations, we only found a decrease in naïve-like $TCF1^+CD45RA^+$ cells in AITL compared to tonsils, but not LN; this was confirmed through supervised analysis (*Online Supplementary Figure S5D*). Collectively, Treg cells were abundant in PTCL and exhibited a high activation profile, suggesting active immunosuppression.

Natural killer cell phenotype is not impaired in peripheral T-cell lymphoma

Natural killer cells are important effectors of the anti-tumor response; nevertheless, their activation and function are often dampened in cancer, constituting an important mechanism of immune escape. We analyzed the distribution and activation / maturation levels of $CD56^+$ NK cells. Unsupervised analyses revealed 6 clusters that could be generally defined as $CD56^{bright}$ cytokine-producing cells, $CD57^+$ cytotoxic cells, and $Ki67^+$ proliferating cells (*Online Supplementary Figure S6A, B*). There was no significant difference in these different populations between control and PTCL samples, with the exception of a slight increase in total $GZMB^+$ cells in AITL, detected through supervised analysis and manual gating (*Online Supplementary Figure S6B-E*). Thus, the PTCL TME did not seem to significantly impact NK-cell distribution.

$CD8^+$ T cells display features of exhaustion

Next, we examined the phenotype of $CD8^+$ T cells in lymphoid tissues. FlowSOM analysis on 17 markers of activation highlighted 18 distinct cell clusters that corresponded to: i) $CD45RA^+$ $TCF1^{+/-}$ naïve-like cells, with low expression of checkpoint molecules; ii) $Ki67^+$ proliferating cells; iii) $GZMB^+$ cells devoid of checkpoint expression; and iv) $CD45RA^-$ activated / memory cells with the expression of at least 2 checkpoint receptors (Figure 3A, B). There were clear differences between tissues (Figure 3C). Differential expression analyses between subgroups of samples, highlighted the loss of naïve-like cells ($CD45RA^+TCF1^+GZMB^-$) in both AITL and PTCL, NOS (clusters 12, 16 and 17) compared to non-malignant tissues (Figure 3B, D). In contrast, $Ki67^+$ cells increased (Figure 1D), and clusters 1, 4, 6 and 7, corresponding to cell subsets with very strong co-expression of PD-1 and TIM-3 among other inhibitory receptors, were significantly enriched in tumor samples. Although variable, the total number of $PD\text{-}1^+TIM\text{-}3^+$ cells was higher in tumor cells compared to tonsils and reactive LN (Figure 3E). Unsupervised clustering efficiently distinguished PTCL from tonsils, but not reactive LN samples, based exclusively on the phenotype of $CD8^+$ T cells (*Online Supplementary Figure S7*). Of note, there were no striking differences in $CD8^+$ T-cell profiles between AITL and PTCL, NOS patients, revealing common features of T-cell immunity between the 2 lymphoma subtypes. We further investigated the phenotype of these cells by performing Boolean analysis following manual gating, and observed a strong increase in cells expressing at least 3 inhibitory receptors in tumor samples compared to healthy tonsils and LN (Figure 3F). This exhausted phenotype, together with the expansion of Treg cells, suggests that strong immune suppression takes place in PTCL lymph nodes, emphasizing the need for immunotherapeutic strategies in these conditions.

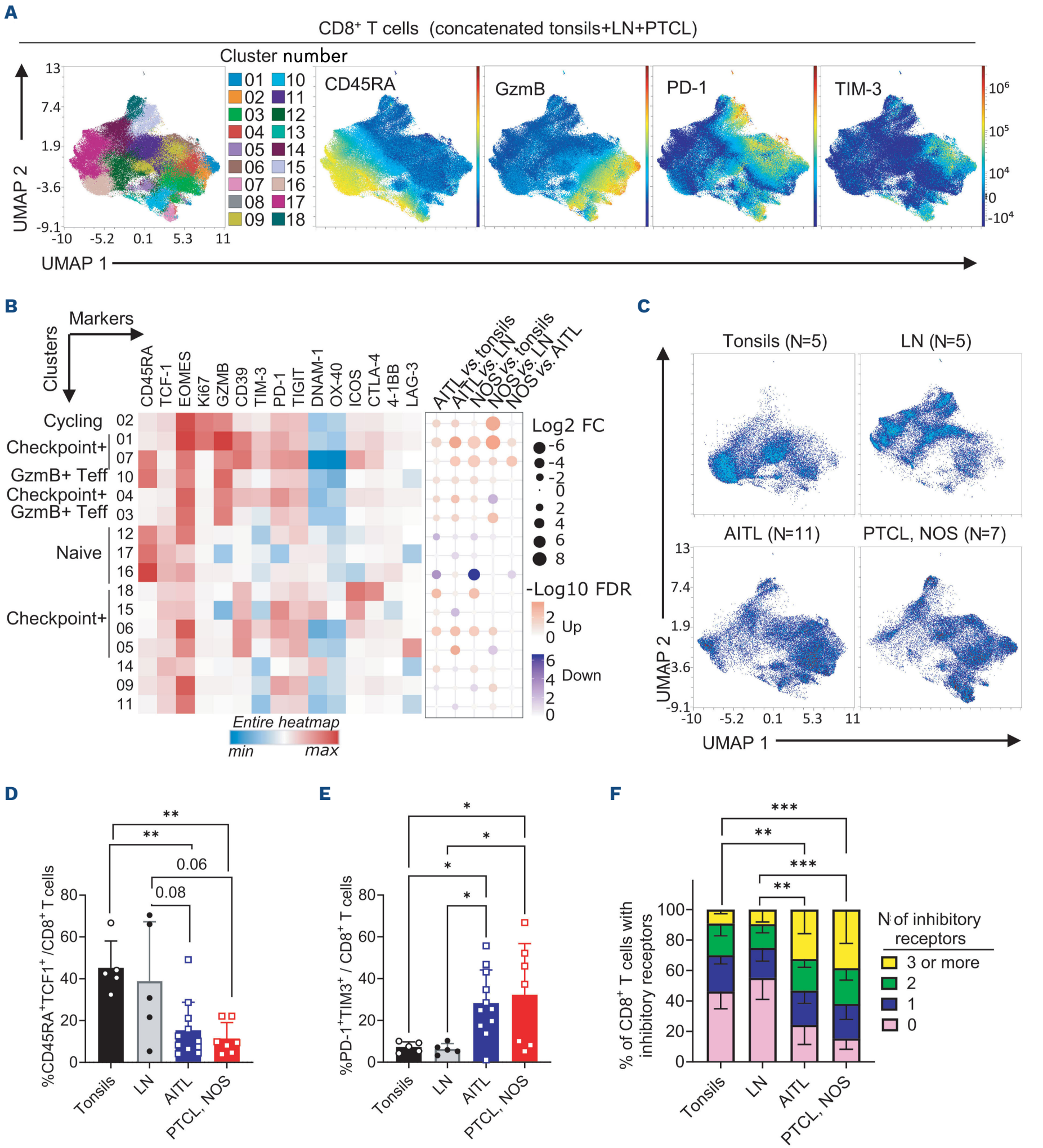

Figure 3. Peripheral T-cell lymphoma-associated CD8⁺ T cells adopt a highly activated, exhausted-like phenotype. (A) UMAP visualization, FlowSOM distribution of clusters and projection of selected markers in concatenated samples, following manual gating on live CD8⁺ T cells and random selection of an equal number of cells between each group. (B) Heatmap showing hierarchical clustering and expression (normalized across markers) of indicated markers in FlowSOM clusters, and their differential enrichment between groups. (C) Distribution of cells from each group on UMAP. (D-F) Proportion of naïve (D) and exhausted (E) CD8⁺ T cells, and Boolean analysis of inhibitory checkpoint-expressing cells (F) upon manual gating. Mean ± Standard Error of Mean is shown; each dot represents a sample. Kruskal-Wallis (D, E) and two-way ANOVA (F) tests were used. FC: flow cytometry; FDR: false discovery rate; LN: lymph nodes; AITL: angioimmunoblastic T-cell lymphoma; PTCL, NOS: peripheral T-cell lymphoma, not otherwise specified. **P*<0.05, ***P*<0.005, ****P*<0.001.

Differential expression of actionable receptors on immune cell subsets

We thus explored whether our strategy may unveil actionable co-stimulatory molecules, i.e., surface checkpoints with specific expression patterns in pro-tumoral subsets (Treg cells and Tconv cells containing tumor cells) *versus* anti-tumoral populations (CD8$^+$ and NK cells). We first analyzed inhibitory checkpoints. As previously described,[18] PD-1 was broadly expressed (an average of 40-60% positive cells) across subsets (NK cells being negative for this receptor, as shown in other contexts[20]) (Figure 4), similarly to TIM-3 (9-57%) and TIGIT (30-70%). Conversely, few cells expressed LAG-3, and CTLA-4 was mostly found on Treg and Tconv cells (18-84% positive cells), while its expression was quite low on CD8$^+$ T cells and NK cells; this was particularly true for AITL samples. In addition, NKG2A was expressed by approximately 50% of NK cells regardless of the pathology, and was undetected on T cells. Concerning 'activation' checkpoints, ICOS and OX-40 followed a pattern similar to CTLA-4, whereas 4-1BB and TNFR2 displayed low expression, the latter being preferentially expressed by Treg cells. Thus, while checkpoint receptors were generally broadly expressed in PTCL, some of these targetable proteins (CTLA-4, ICOS, OX-40) showed specific expression patterns with high expression in Tconv (including tumor cells) and Treg cells, and low expression in anti-tumor effectors, indicating that they may be considered therapeutic targets.

Increased CD39 expression in peripheral T-cell lymphoma is associated with poor prognosis

In addition to these checkpoints, belonging to the CD28 and tumor necrosis factor receptor superfamilies, we also investigated the expression levels of the ectonucleoti-

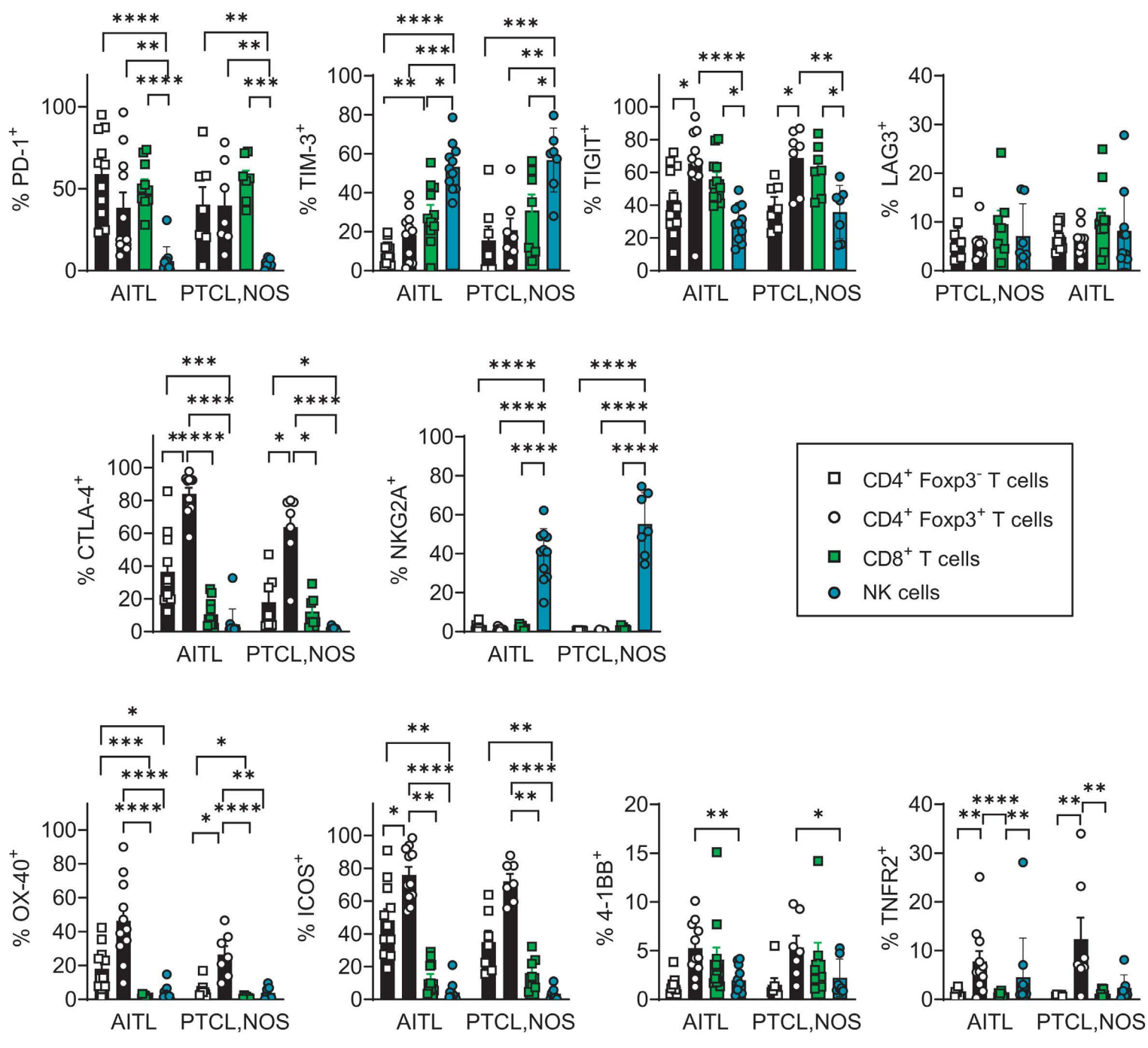

Figure 4. Differential expression pattern of checkpoint receptors on immune subsets in peripheral T-cell lymphoma. Proportion of checkpoint-expressing cells in different cell subsets following manual gating is shown as Mean ± Standard Error of Mean. Two-way ANOVA tests were used. AITL: angioimmunoblastic T-cell lymphoma; PTCL, NOS: peripheral T-cell lymphoma, not otherwise specified; NK: natural killer cells. *P<0.05, *P<0.005, ***P<0.001, ****P<0.0001. Non-significant values are not displayed.

dase CD39. CD39 is a surface protein that has recently emerged as an important immune checkpoint in cancer through its ability to convert ATP to AMP, ultimately leading to the production of the immunosuppressive nucleoside adenosine.[21] While CD39 was mostly expressed by DC, B cells, and NK cells in tonsils and non-tumoral LN, it was expressed by some T cells in PTCL patients (Figure 5A, B). In CD8$^+$ T cells, CD39 was largely enriched in activated cells compared to naïve cells, and, to a greater extent, in exhausted T cells (*Online Supplementary Figure S8A*). To investigate whether this tumor-specific CD39 expression by T cells was associated with other immune perturba-

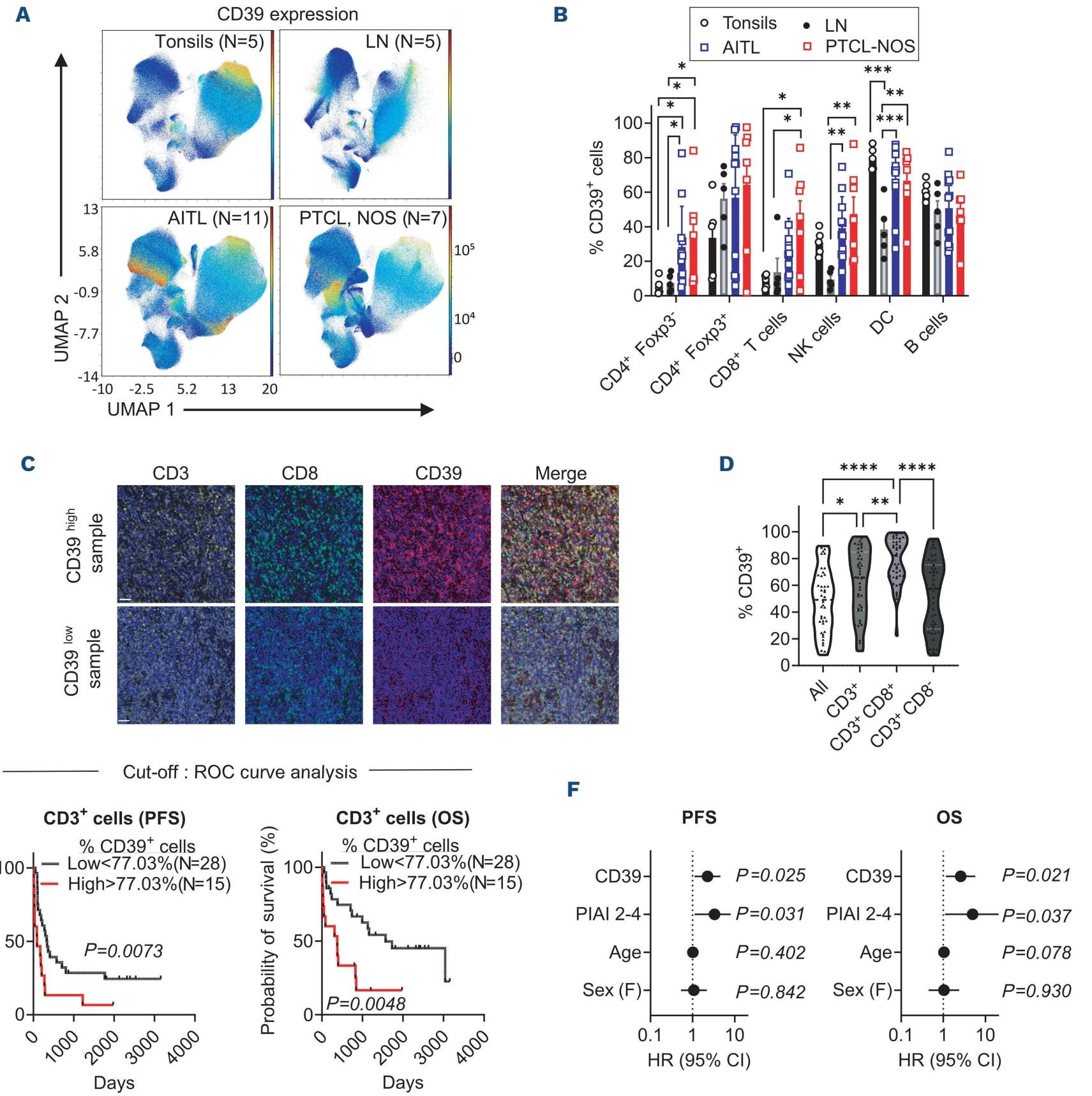

Figure 5. CD39 expression and prognostic value in peripheral T-cell lymphoma. (A) UMAP visualization of CD39 expression across samples. (B) Proportion of CD39$^+$ cells across subsets and samples following manual gating. (C) Representative multi-immunofluorescence (multi-IF) staining in a CD39^{high} (top) and a CD39^{low} (bottom) sample. (D) Multi-IF quantification of CD39$^+$ cells across subsets and samples. (E) Kaplan-Meier curves of progression-free survival (PFS) and overall survival (OS). CD39^{high} and CD39^{low} samples were split upon Receiver Operating Characteristic (ROC) curve analyses (F), Hazard Ratio (HR, dots), and 95% Confidence Interval values (CI, bars) of the different parameters used in multivariate analyses. Two-way ANOVA (B, D), log-rank (E), and multivariate Cox regression (F) tests were used. LN: lymph nodes; AITL: angioimmunoblastic T-cell lymphoma; PTCL, NOS: peripheral T-cell lymphoma, not otherwise specified; F: female. *P<0.05, **P<0.005, ***P<0.001, ****P<0.0001.

tions, we split our 18-sample cohort into CD39 low, intermediate and high groups (*Online Supplementary Figure S8B*). No correlation with major immune subtypes could be found (*Online Supplementary Figure S8C*). Interestingly, increase in CD39 expression was associated with enhanced TIM-3/PD-1 and CTLA-4$^+$CD8$^+$ T-cell subsets, although this did not reach significance (*Online Supplementary Figure S8D*). Conversely, high CD39 expression was correlated with lower GZMB expression, likely to be indicative of immune dysfunction sustaining tumor progression. We thus wondered whether CD39 expression impacted PTCL clinical outcome. First, we investigated the putative prognostic value of CD39 at the RNA level in bulk samples by examining the association between *ENTPD1* expression and OS in the TENOMIC cohort, that consists of a dataset of microarray-defined gene expression profiles of 85 LN samples of AITL patients. In this cohort, the level of *ENTPD1* expression in the whole bulk of cells was not significantly associated with a prognostic value (*Online Supplementary Figure S8E*). To further explore the expression of CD39 at the protein level in T-cell subsets, we used a multi-immunofluorescence (IF) approach on tissue microarrays (TMA) comprising 43 LN samples from AITL patients at diagnosis, with a 10-year clinical history (*Online Supplementary Tables S3 and S4*). PFS and OS in the cohort matched previously reported data (*Online Supplementary Figure S8F*). Slides were stained for CD3, CD8, CD39, and DAPI, and the proportion of each population was determined. CD3$^+$ T cells, in particular the CD8$^+$ subset, exhibited higher CD39 expression compared to non-T cells. As in FACS analyses, we observed an important variability in CD39 expression between patients (Figure 5C, D). We first measured the impact of CD39 expression in different subsets by splitting the samples based on the median expression of CD39. Although the proportion of CD39$^+$ cells among all cells was not associated with prognostic significance, patients harboring high CD39 expression among T cells (regardless of CD8 expression) showed a trend toward poorer prognosis (*Online Supplementary Figure S8G*). To refine this analysis, we analyzed the data following Receiver Operating Characteristic (ROC) curve-based separation of patients. We found that patients harboring the highest expression of CD39 in T cells (N=15, 35% of the entire cohort) exhibited a significantly poorer prognosis, both at the PFS and OS levels (Figure 5E). Similar conclusions were reached when analyzing CD39 expression in the CD3$^+$CD8$^+$ and CD3$^+$CD8$^-$ subsets (*Online Supplementary Figure S8H*). The prognostic value of CD39 expression by T cells was further confirmed through multivariate Cox models including Prognostic Index for AITL (PIAI), sex, and age (Figure 5F). Together, our data suggest CD39 expression by T cells may represent a novel independent prognostic factor in AITL and should be explored as a putative target.

Discussion

To date, and in contrast to many solid tumors and other hematologic malignancies, there is a clear lack of knowledge in the distribution and phenotype of immune cells in the context of PTCL. Our study documents an accumulation of highly activated and heterogeneous T-cell populations, whereas B-cell populations were less abundant in this disease. Although this confirms recently reported data,[18] this does not preclude the therapeutic targeting of B cells, as these can support tumor cells.[22,23]

One striking observation that can be made based on our data is the large phenotypic heterogeneity of Tconv cells between PTCL patients. Although most Tconv cells expressed at least one checkpoint surface receptor, only about half of them expressed PD-1 or ICOS, suggesting that the phenotype and biology of AITL cells extend beyond these 2 single markers. This merits further exploration; for example, by combining high-dimensional cytometry to single-cell TCR-seq that allows the identification of clonal cell populations. Most CD8$^+$ T cells in both AITL and PTCL, NOS expressed at least one inhibitory checkpoint and a prominent PD-1$^+$TIM3$^+$ population could be detected, suggesting that an active exhaustion process might be taking place in PTCL tissues. This is in accordance with observations made in patients with cutaneous T-cell lymphoma and other non-Hodgkin lymphomas,[24-26] and confirms the potential benefit of checkpoint-based immunotherapies in PTCL.

In this regard, we aimed to identify surface receptors expressed by cytotoxic T cells and/or NK cells but not by Tconv cells (that included most malignant cells) and Treg cells, or vice versa. Similar to the large spectrum of PD-1 expression (that may explain the hyperprogression detected in some PTCL patients following PD-1 blockade), we observed that TIGIT and TIM-3 were largely expressed by both tumor-promoting (tumor cells, Treg cells) and tumor-inhibiting (CD8$^+$ T cells, NK cells) populations. This broad expression may negate the therapeutic potential of blocking Ab, that are currently under clinical development in solid and hematologic malignancies.[27] In contrast, other surface markers, such as OX-40, or, to a lesser extent, CTLA-4 or ICOS, displayed a much higher expression on CD4$^+$ (comprising tumor cells and Treg cells) than other subsets. These may thus represent attractive therapeutic targets for the treatment of PTCL. In line with this, mRNA expression of *CTLA4* was shown to be associated with poor prognosis in a meta-analysis of PTCL transcriptomes.[28] Specifically, this would require the use of depleting monoclonal Ab (mAb) through the use of Ab-dependent cellular cytotoxicity and phagocytosis-optimized IgG1 molecules.[29] To date, and to our knowledge, OX-40 mAb under development have agonistic functions and should not be recommended for the treatment of PTCL. The depleting effect of current anti-CTLA-4 mAb, such as ipilimumab, is still a subject of

wide debate and there is room for improvement.[30,31] Different strategies have been used to create anti-CTLA4 IgG1 mAb with strong Treg-depleting properties and anti-tumor effects in preclinical models[32,33] which deserve attention for PTCL therapy. MEDI-570, an afucosylated IgG1 anti-ICOS mAb, was shown to induce T-cell depletion in cynomolgus monkeys;[34] a phase I trial reported positive signs of activity in AITL patients.[35] In addition to these T-cell-targeting agents, NKG2A also appears to be an interesting target in PTCL as its expression was largely restricted to NK cells. As blocking anti-NKG2A mAb are currently under clinical evaluation in solid cancers,[36] they may represent a future therapeutic avenue in PTCL.

In addition to these traditional immune checkpoints, our data highlight CD39 as a promising target in nodal PTCL, both through its prognostic value and its potential therapeutic targeting. The combined action of CD39 and CD73 that leads to the production of adenosine have been extensively described for their tumor-promoting functions in solid cancers.[21] CD39 inhibition reinvigorates cytotoxic T-cell activity in preclinical models of melanoma or sarcoma, among others.[37] CD39 expression also increases in different hematologic malignancies, including T-cell-derived cancers such as adult T-cell leukemia / lymphoma or Sezary syndrome.[38,39] High expression of CD39 was shown to be associated with poor prognosis in diffuse large B-cell lymphoma and multiple myeloma.[40,41] CD39 expression on T cells is correlated with disease severity in patients with chronic lymphocytic leukemia.[42,43] Because of this association with tumor progression, the therapeutic potential of CD39 inhibition has mainly been evaluated in blood cancers. For example, mAb targeting CD39 potentiate the therapeutic efficacy of T-cell transfer in a humanized model of B-cell lymphoma,[44] whereas ARL67156 and POM-1, two ectonucleotisase inhibitors with high affinity for CD39, enhance T-cell function in follicular lymphoma and multiple myeloma patient samples, respectively.[41,45] CD73 or A2AR inhibition enhances non-tumoral T-cell proliferation in Sezary syndrome *in vitro*.[46] Our data now extend the tumor-promoting properties of CD39 to nodal PTCL. We propose that CD39 expression could be assessed by immunohistochemistry and/or flow cytometry as a potent prognostic factor in AITL. Moreover, patients with PTCL may benefit from the CD39-blocking agents currently under clinical development for other cancers.

Disclosures

EM reports research funding from Astra-Zeneca. PG reports consultancy for Gilead and Takeda, and research funding from Alderan, Innate Pharma, Sanofi, and Takeda. FL reports research funding from Institut Roche and travel grant from Gilead. LdL reports consultancy for AbbVie, Bayer, Bio Ascend, Lunaphore, Novartis. EB reports consultancy or lecture fees from Incyte, Roche, Takeda, ADCTherapeutics, Novartis, Kite/GILEAD, Miltenyi, Janssen, and Sanofi, travel expense reimbursement from Roche, Gilead, and Abbvie, and research funding from Agmen, Bristol-Myers Squibb, and Daiichi Sankyo. PSu reports consultancy or lecture fees from Gilead/Kyte, Janssen Cylag, BMS/Cellgene, and Abbvie, and research funding from Astra-Zeneca and Servier. The other authors have no conflicts of interest to disclose.

Contributions

PSt, JP, AV, MBarb, TA, MBard and GT performed experiments and analyzed data. MP, MG, JC, EM, PG, LDL, EB, LG and YGB analyzed data. PG, FL, LDL, EB, PSu, LG and ATG selected patient samples and confirmed the original diagnosis through pathological analyses. YGB supervised the study, wrote the paper, and secured funding.

Acknowledgments

We thank the CeVi_Collection group (https://experts-recherche-lymphome.org/calym/explorer-les-ressources-du-consortium/collection-cevi/centres-participants-a-la-collection-cevi/) from the CALYM Carnot Institute funded by the French National Research Council (ANR) for providing cell suspension samples from PTCL patients. We thank the biological resource centers of Montpellier, Toulouse, and Creteil for providing the fixed tissue samples obtained at diagnosis, used for re-assessment of the original diagnosis. We are grateful to Maud Plaschka (CCRI, Vienna, Austria) for bioinformatics analyses. We thank Pierre Milpied (CIML, Marseille, France), as well as all members of the lab, for helpful discussions on the project.

Funding

This project was funded by grants from la Ligue contre le Cancer, the ATIP-Avenir funds, and the Laboratory of Excellence (LabEx) Dev2Can (ANR-10-LABX-0061), to YGB. PS was supported by a scholarship from the Fondation pour la Recherche Médicale (FRM). AV was supported by a fellowship from the Association pour la Recherche contre le Cancer (ARC) Foundation.

Data-sharing statement

All raw or analyzed data will be made available upon reasonable request by e-mail to the corresponding author.

References

1. Campo E, Jaffe ES, Cook JR, et al. The International Consensus Classification of Mature Lymphoid Neoplasms: a report from the Clinical Advisory Committee. Blood. 2022;140(11):1229-1253.
2. Fujisawa M, Chiba S, Sakata-Yanagimoto M. Recent progress in the understanding of angioimmunoblastic T-cell lymphoma. J Clin Exp Hematop. 2017;57(3):109-119.

3. de Leval L, Parrens M, Le Bras F, et al. Angioimmunoblastic T-cell lymphoma is the most common T-cell lymphoma in two distinct French information data sets. Haematologica. 2015;100(9):e361-364.
4. Armand P, Shipp MA, Ribrag V, et al. Programmed death-1 blockade with pembrolizumab in patients with classical Hodgkin lymphoma after brentuximab vedotin failure. J Clin Oncol. 2016;34(31):3733-3739.
5. Ansell SM, Lesokhin AM, Borrello I, et al. PD-1 blockade with nivolumab in relapsed or refractory Hodgkin's lymphoma. N Engl J Med. 2015;372(4):311-319.
6. Bennani NN, Kim HJ, Pederson LD, et al. Nivolumab in patients with relapsed or refractory peripheral T-cell lymphoma: modest activity and cases of hyperprogression. J Immunother Cancer. 2022;10(6):e004984.
7. Shi Y, Wu J, Wang Z, et al. Efficacy and safety of geptanolimab (GB226) for relapsed or refractory peripheral T cell lymphoma: an open-label phase 2 study (Gxplore-002). J Hematol Oncol. 2021;14(1):12.
8. Ratner L, Waldmann TA, Janakiram M, Brammer JE. Rapid progression of adult T-cell leukemia-lymphoma after PD-1 inhibitor therapy. N Engl J Med. 2018;378(20):1947-1948.
9. Wartewig T, Kurgyis Z, Keppler S, et al. PD-1 is a haploinsufficient suppressor of T cell lymphomagenesis. Nature. 2017;552(7683):121-125.
10. Wilcox RA, Wada DA, Ziesmer SC, et al. Monocytes promote tumor cell survival in T-cell lymphoproliferative disorders and are impaired in their ability to differentiate into mature dendritic cells. Blood. 2009;114(14):2936-2944.
11. Ham JS, Park HY, Ryu KJ, Ko YH, Kim WS, Kim SJ. Elevated serum interleukin-10 level and M2 macrophage infiltration are associated with poor survival in angioimmunoblastic T-cell lymphoma. Oncotarget. 2017;8(44):76231-76240.
12. Sugio T, Miyawaki K, Kato K, et al. Microenvironmental immune cell signatures dictate clinical outcomes for PTCL-NOS. Blood Adv. 2018;2(17):2242-2252.
13. Zhu Q, Deng X, Yao W, et al. Novel tumour-infiltrating lymphocyte-related risk stratification based by flow cytometry for patients with de novo angioimmunoblastic T cell lymphoma. Ann Hematol. 2021;100(3):715-723.
14. Chen Z, Zhu Q, Deng X, et al. Angioimmunoblastic T-cell lymphoma with predominant CD8+ tumor-infiltrating T-cells is a distinct immune pattern with an immunosuppressive microenvironment. Front Immunol. 2022;13:987227.
15. Ohue Y, Nishikawa H. Regulatory T (Treg) cells in cancer: can Treg cells be a new therapeutic target? Cancer Sci. 2019;110(7):2080-2089.
16. Lundberg J, Berglund D, Molin D, Kinch A. Intratumoral expression of FoxP3-positive regulatory T-cells in T-cell lymphoma: no correlation with survival. Ups J Med Sci. 2019;124(2):105-110.
17. Bruneau J, Canioni D, Renand A, et al. Regulatory T-cell depletion in angioimmunoblastic T-cell lymphoma. Am J Pathol. 2010;177(2):570-574.
18. Pritchett JC, Yang ZZ, Kim HJ, et al. High-dimensional and single-cell transcriptome analysis of the tumor microenvironment in angioimmunoblastic T cell lymphoma (AITL). Leukemia. 2022;36(1):165-176.
19. Gaulard P, de Leval L. Follicular helper T cells: implications in neoplastic hematopathology. Semin Diagn Pathol. 2011;28(3):202-213.
20. Judge SJ, Dunai C, Aguilar EG, et al. Minimal PD-1 expression in mouse and human NK cells under diverse conditions. J Clin Invest. 2020;130(6):3051-3068.
21. Moesta AK, Li XY, Smyth MJ. Targeting CD39 in cancer. Nat Rev Immunol. 2020;20(12):739-755.
22. Fujisawa M, Nguyen TB, Abe Y, et al. Clonal germinal center B cells function as a niche for T-cell lymphoma. Blood. 2022;140(18):1937-1950.
23. Delfau-Larue MH, de Leval L, Joly B, et al. Targeting intratumoral B cells with rituximab in addition to CHOP in angioimmunoblastic T-cell lymphoma. A clinicobiological study of the GELA. Haematologica. 2012;97(10):1594-1602.
24. Querfeld C, Leung S, Myskowski PL, et al. Primary T cells from cutaneous T-cell lymphoma skin explants display an exhausted immune checkpoint profile. Cancer Immunol Res. 2018;6(8):900-909.
25. Heming M, Haessner S, Wolbert J, et al. Intratumor heterogeneity and T cell exhaustion in primary CNS lymphoma. Genome Med. 2022;14(1):109.
26. Yang ZZ, Liang AB, Ansell SM. T-cell-mediated antitumor immunity in B-cell non-Hodgkin lymphoma: activation, suppression and exhaustion. Leuk Lymphoma. 2015;56(9):2498-2504.
27. Ansell SM, Lin Y. Immunotherapy of lymphomas. J Clin Invest. 2020;130(4):1576-1585.
28. Li X, Liu Z, Mi M, et al. Identification of hub genes and key pathways associated with angioimmunoblastic T-cell lymphoma using weighted gene co-expression network analysis. Cancer Manag Res. 2019;11:5209-5220.
29. Yu J, Song Y, Tian W. How to select IgG subclasses in developing anti-tumor therapeutic antibodies. J Hematol Oncol. 2020;13(1):45.
30. Sharma A, Subudhi SK, Blando J, et al. Anti-CTLA-4 immunotherapy does not deplete FOXP3(+) regulatory T cells (Tregs) in human cancers-Response. Clin Cancer Res. 2019;25(11):3469-3470.
31. Quezada SA, Peggs KS. Lost in translation: deciphering the mechanism of action of anti-human CTLA-4. Clin Cancer Res. 2019;25(4):1130-1132.
32. Ha D, Tanaka A, Kibayashi T, et al. Differential control of human Treg and effector T cells in tumor immunity by Fc-engineered anti-CTLA-4 antibody. Proc Natl Acad Sci U S A. 2019;116(2):609-618.
33. Semmrich M, Marchand JB, Fend L, et al. Vectorized Treg-depleting alphaCTLA-4 elicits antigen cross-presentation and CD8(+) T cell immunity to reject 'cold' tumors. J Immunother Cancer. 2022;10(1):e003488.
34. Nicholson SM, Carlesso G, Cheng LI, et al. Effects of ICOS+ T cell depletion via afucosylated monoclonal antibody MEDI-570 on pregnant cynomolgus monkeys and the developing offspring. Reprod Toxicol. 2017;74:116-133.
35. Chavez JC, Foss FM, MD, William BM, et al. A phase I study of anti-ICOS antibody MEDI-570 for relapsed / refractory (R/R) peripheral T-cell lymphoma (PTCL) and angioimmunoblastic T-cell lymphoma (AITL) (NCI-9930). Blood. 2020;136(Suppl 1):5-6.
36. van Hall T, Andre P, Horowitz A, et al. Monalizumab: inhibiting the novel immune checkpoint NKG2A. J Immunother Cancer. 2019;7(1):263.
37. Perrot I, Michaud HA, Giraudon-Paoli M, et al. Blocking antibodies targeting the CD39/CD73 immunosuppressive pathway unleash immune responses in combination cancer therapies. Cell Rep. 2019;27(8):2411-2425.e9.
38. Nagate Y, Ezoe S, Fujita J, et al. Ectonucleotidase CD39 is highly expressed on ATLL cells and is responsible for their immunosuppressive function. Leukemia. 2021;35(1):107-118.
39. Bensussan A, Janela B, Thonnart N, et al. Identification of CD39 as a marker for the circulating malignant T-cell clone of Sezary

syndrome patients. J Invest Dermatol. 2019;139(3):725-728.
40. Nakamura K, Casey M, Oey H, et al. Targeting an adenosine-mediated “don’t eat me signal” augments anti-lymphoma immunity by anti-CD20 monoclonal antibody. Leukemia. 2020;34(10):2708-2721.
41. Yang R, Elsaadi S, Misund K, et al. Conversion of ATP to adenosine by CD39 and CD73 in multiple myeloma can be successfully targeted together with adenosine receptor A2A blockade. J Immunother Cancer. 2020;8(1):e000610.
42. Perry C, Hazan-Halevy I, Kay S, et al. Increased CD39 expression on CD4(+) T lymphocytes has clinical and prognostic significance in chronic lymphocytic leukemia. Ann Hematol. 2012;91(8):1271-1279.
43. Aroua N, Boet E, Ghisi M, et al. Extracellular ATP and CD39 activate cAMP-mediated mitochondrial stress response to promote cytarabine resistance in acute myeloid Leukemia. Cancer Discov. 2020;10(10):1544-1565.
44. Li XY, Moesta AK, Xiao C, et al. Targeting CD39 in cancer reveals an extracellular ATP- and inflammasome-driven tumor immunity. Cancer Discov. 2019;9(12):1754-1773.
45. Hilchey SP, Kobie JJ, Cochran MR, et al. Human follicular lymphoma CD39+-infiltrating T cells contribute to adenosine-mediated T cell hyporesponsiveness. J Immunol. 2009;183(10):6157-6166.
46. Sonigo G, Bozonnat A, Dumont M, et al. Involvement of the CD39/CD73/adenosine pathway in T-cell proliferation and NK cell-mediated antibody-dependent cell cytotoxicity in Sezary syndrome. Blood. 2022;139(17):2712-2716.